# Characterization of Microcrystalline Cellulose after Pretreatment with Low Concentrations of Ionic Liquid-$H_2O$ for a Pyrolysis Process

Qiyu Chen, Takumi Endo, Qingyue Wang*

Microcrystalline cellulose (MCC) samples pretreated by ionic liquid (ILs)-$H_2O$ mixtures were studied for application in a pyrolysis process. A 1-ethyl-3-methylimidazolium methanesulfonate [Emim][$MeSO_3$]-$H_2O$ mixture with solid acid catalyst Nafion®NR50 was used in the pretreatment process. A lower amount of hydrogen bonding between neighboring pretreated MCC chains resulted from a less ordered cellulose structure, leading to lower crystallinity, decreased molecular weight and reduced thermal stability. The pyrolysis result showed that the yields of char were lower, the average reaction rate increased, and the DTG peak temperature decreased relative to the untreated MCC. The amount and concentration of the hydrogen gas obtained from the pyrolysis of sample 90(20) (4.00 mmol/g-sample) was higher than that obtained from the pyrolysis of the MCC (3.26 mmol/g-sample). This study explores MCC (pretreated by ionic liquid-$H_2O$ mixtures) with a recyclable solid acid catalyst under varying pretreatment conditions, as a potential raw feed material, to be applied in the pyrolysis process.

*Keywords: Microcrystalline cellulose; Ionic liquid-$H_2O$; Pretreatment; Pyrolysis; Gaseous products*

*Contact information: Laboratory for Circulation and Control of Environmental Chemicals, Graduate School of Science and Engineering, Saitama University, Shimo-Okubo 255, Sakura-ku, Saitama City 3388570, Japan; *Corresponding author: seiyo@mail.saitama-u.ac.jp*

## INTRODUCTION

Cellulose, as an abundant raw material consisting of renewable polysaccharides, can enter the biorefinery for the production of an array of products, including transportation fuels and other products, to meet world energy needs. Cellulose is a high molecular weight linear-polymer composed of D-glucopyranose units linked by β-1,4-glycosidic bonds. Three hydroxyl groups are able to interact with one another forming intramolecular (O3′-H…O5; O2-H…O6′) and intermolecular (O6′-H…O3) hydrogen bonds in each of the glucopyranose units. Cellulose does not dissolve in water or in some aprotic solvents such as alcohols and amines. Some solvents including lithium chloride/dimethylacetamide (LiCl/DMAc), N-methylmorpholine-N-oxide monohydrate aqueous solutions, and metal complexes (NMMO) that were applied in the study of dissolving cellulose and cellulose derivatives suffer from toxicity, recycling problems, and thermal instability (Olivier-Bourbigou *et al*. 2010). Since Swatloski *et al*. (2002) reported that cellulose could dissolve in ionic liquid, many studies had been focused on the subject of lignocellulosic biomass conversion. The search for new ILs for dissolving and processing cellulose has attracted increasing attention (Pinkert *et al*. 2009; Gericke *et al*. 2013). The chemical and physical pretreatment of biomass resources is a field of growing interest and practicality (Mosier *et al*. 2005). The pretreatment of cellulose materials can affect their physical properties such

as crystallinity, surface structure and area, and degree of polymerization. These changes, such as enzymatic hydrolysis can affect their subsequent utilization (Brandt *et al*. 2013).

Recently, ionic liquid-$H_2O$ (IL-$H_2O$) pretreatment methods have been of considerable interest, and pretreated samples have been used in subsequent applications, such as saccharification or enzymatic dehydrogenation (Sun *et al*. 2009; Li *et al*. 2010). Adding water or other organic solvents to IL systems can reduce the processing cost significantly and allow the large-scale treatment of cellulose. The effect of pH value (Zhang *et al*. 2013), particle size (Bahcegul *et al*. 2012; Hou *et al*. 2013), water content, pretreatment time, and other influencing factors (Brandt *et al*. 2011) have been investigated based on lignocellulosic biomass research. Generally, the more water in an IL-$H_2O$ mixture system, the less the concentration of cellulose in the solution (Mazza *et al*. 2009), due to the water molecules binding to two anions by hydrogen bonds (López-Pastor *et al*. 2006). Thus, it appears to be difficult to achieve the total dissolution of biomass in an IL-$H_2O$ mixture.

The pyrolysis process is a thermochemical reaction method used in developing clean energy. Products of pyrolysis have been investigated as a substitute for fossil resources. Pyrolysis refers to the thermal decomposition of a material to form some combination of gaseous products (*e.g*., $H_2$, CO, $CO_2$, $CH_4$ and hydrocarbons), liquids (tar and water), and solids (char) (Yang *et al*. 2006). Approaches for biomass conversion that involve pyrolysis include fast pyrolysis, gasification, and catalytic fast pyrolysis.

The proposed methods for transforming biomass into useful products are the microbial fermentation method, saccharification of the glucose and other carbohydrates, and thermo-chemical conversion of the lignocellulose biomass by a pyrolysis or gasification process. One important tool in reducing the cost of this depolymerization is the pretreatment of the lignocellulosics to make the biomass matrix more accessible to these applications. As an important pretreatment method, pretreatment of lignocellulosic materials by an IL-$H_2O$ mixture has recently generated much interest (Chen *et al*. 2015). This study explores the significance of ionic liquids as pretreatment solvents with water and a recyclable solid acid catalyst. As a possible mechanism it is suggested that the water hydrogen-bonds strongly to the ionic liquid's anion, so reducing its propensity to interact with the cellulose. It also prevents the coordination of ionic liquid anions to the cellulose. The anion from ILs were released due to the ion-exchange with the sulfonate ($SO_3H$) groups, meanwhile, the released $H^+$ from solid acid which interacting with the hydroxyl group of cellulose. After the pretreatment process, the pretreated microcrystalline cellulose (MCC), as a potential raw feed material, was applied in the pyrolysis process with a focus on the pyrolysis kinetics and gaseous products. In addition, the characterization of MCC in a crystalline structure or a decomposition rate effect on the cellulose pyrolysis process could be expected due to a quantitative assessment of the IL-$H_2O$ mixture pretreatment system.

The 1-ethyl 3-methylimidazolium methylsulfonate [Emim][$MeSO_3$]- $H_2O$ mixtures have been investigated as green solvents for the pretreatment process (Heym *et al*. 2011). The use of macroreticulated styrene-divinylbenzene resins functionalized with sulfonic groups to catalyze the hydrolysis has been previously reported (Rinaldi *et al*. 2008). The solid acid catalyst Nafion®NR50 with good thermal stability was loaded in the IL-$H_2O$ mixture system to promote a more efficient pretreatment process in a lower concentration ionic liquid at a lower reaction temperature for economic reasons.

In this work, the MCC pretreated under different conditions was characterized by X-ray diffraction (XRD), Fourier transform infrared spectroscopy (FTIR), gel permeation

chromatography (GPC), and scanning electron microscopy (SEM) for extensive structural feature determination. Thermogravimetric and differential thermal analysis (TG-DTA) was employed to understand the relative changes in the pyrolysis rate and solid product. The gaseous products were determined by a gas chromatograph equipped with a thermal conduct detector (GC-TCD) and a gas chromatograph equipped with a flame ionization detector (GC-FID). This study could play a role as a bridge a gap in the pretreatment process of pyrolysis for operational applications.

## EXPERIMENTAL

### Materials and Chemicals

Microcrystalline cellulose (MCC, *ca*. 0.05 mm) samples were supplied by SERVA Electrophoresis GmbH (Germany). The MCC was further dried in a vacuum oven at 105 °C to eliminate the moisture content. The proximate analysis of the MCC was carried out based on the JIS-M8812 standard and it resulted in moisture, volatile matter, fixed carbon and ash contents of 7.2, 86.9, 5.9 and 0.0 wt. %, respectively. The total 43.3 wt.% C, 50.46 wt.% O, 6.2 wt.% H, and 0.0 wt.% N concentrations were determined using a CHN coder (Yanagimoto MT-5) based on JIS-M8813. The ionic liquid 1-ethyl-3-methylimidazolium methanesulfonate ([Emim][$MeSO_3$], $C_7H_{14}N_2O_3S$, purity ≥95%; impurities ≤0.5% water) is a product of BASF and was supplied by Sigma-Aldrich (USA). The solid acid catalyst Nafion®NR50 (NR50, ≥0.8 meq/g ion exchange capacity) supplied by Sigma-Aldrich (USA). All other chemicals were reagent grade, purchased from Wako Pure Chemical Industries (Japan) and used without further purification.

### Methods

*Pretreatment process*

MCC powder was loaded into a flask, and then the selected ionic liquid, [Emim][$MeSO_3$], deionized water, and NR50 were added (mass ratio of MCC sample to ionic liquid, $H_2O$, and solid acid catalyst was 1 : 5 : (0.25, 0.5, 1, 2.5, and 5) : 0.5) at 90, 120, and 150 °C for 60 min. The flask was heated and stirred while immersed in an oil bath. The pretreated samples were washed with methanol and deionized water to remove the ionic liquid mixtures. The solid acid catalyst NR50, with a larger granule size than the MCC powder particle size, was removed by manual separation. The pretreated MCC samples were dried in a vacuum oven at 105 °C for 24 h for subsequent analysis and pyrolysis experiments.

*Analytical methods*

The X-ray diffraction (XRD) experiments were performed on an Ultima III X-Ray diffractometer (Rigaku Co. Ltd., Japan). Ni-filtered Cu K α radiation ($\lambda$=0.1542 nm) was generated from 40 kV voltage and 40 mA current. The range of intensities was from 10° to 40° with a 2°/min scan speed. The crystallinity index (Cr.I.) was determined by the Segal method (Wada *et al*. 2001).

The crystalline index was calculated using Eq. 1,

$$\text{Cr. I.} = \frac{I_{002} - I_{am}}{I_{002}} \times 100 \quad (1)$$

where $I_{002}$ is the height of the 002 peak and $I_{am}$ is the height of the minimum between the 002 and the 101 peaks.

The *d*-spacings were calculated using Eq. 2,

$$d_{002} = \frac{\lambda}{2\sin\theta} \quad (2)$$

where $\lambda$ is the X-ray wavelength (0.1542 nm), and $\theta$ is the Bragg angle corresponding to the (002) plane.

The pretreated MCC was analyzed by a Fourier transform infrared spectroscope (FTIR, Model IR-6100, Jasco Co. Ltd., Japan). The ratio of the samples to spectroscopic grade KBr was 1:100; all of the infrared spectra were recorded in absorbance units within the range of 4000 to 400 $cm^{-1}$. The nitrocellulose was dissolved in tetrahydrofuran (THF) to evaluate the average molecular weight. The molecular weight distribution was determined by a gel permeation chromatography system equipped with KF-G and KD806L gel columns (Shodex, Showa Denko K.K. Co. Ltd., Japan) and nitrocellulose with a ratio of 0.1% (w/v) and filtered through a 0.45 μm membrane. The surface morphological changes of MCC and pretreated samples were observed by a scanning electron microscope (SEM, Model S-2400, Hitachi Co. Ltd., Japan) under an acceleration voltage of 15kV.

*Pyrolysis process and analytical methods*

The pyrolysis experiments were performed in a vertical tubular fixed-bed reactor. The temperature was measured by a thermocouple inside the bed. In each experiment, unless otherwise noted, 1.0 g samples were placed into the bottom of the reactor, and 5.0 g mixed $SiO_2/Ca(OH)_2$ catalyst was placed into the top of the reactor at 800 °C. The experiment was carried out with a heating rate of 10 K/min, and the samples were heated from room temperature to 900 °C under argon gas with a flow rate of 70 mL/min. The liquid phase consisted of oil and water phases that were separated and weighed. The four major gases, including $H_2$, CO, $CH_4$, and $CO_2$, were measured by a gas chromatograph equipped with a thermal conduct detector (GC-TCD, Model GC-2014, Shimadzu Co. Ltd., Japan). The hydrocarbon gases, including $C_2H_6$, $C_2H_4$, $C_3H_8$, and $C_3H_6$ were analyzed on a gas chromatograph equipped with a flame ionization detector (GC-FID, Model GC-2010, Shimadzu Co. Ltd., Japan). The char yields were calculated by thermogravimetric and differential thermal analysis (TG-DTA) (Model DTG-60, Shimadzu Co. Ltd., Japan). Approximately 10 mg of the sample was placed on the scale in the apparatus, and the sample was heated up to 900 °C under an Ar atmosphere.

The decomposition rate of MCC is generally described as follows Eq. 3,

$$\frac{d\alpha}{dt} = k(T)f(\alpha) \quad (3)$$

where $\alpha$ is the conversion degree, $T$ is the rate constant dependent on the pyrolysis temperature, and $f(\alpha)$ is a conversion function dependent on the pyrolysis reaction mechanism.

The fractional conversion $\alpha$ is expressed as Eq. 4,

$$\alpha = \frac{(m_0 - m)}{(m_0 - m_\infty)} \quad (4)$$

where $m_0$ is the initial weight of the sample, $m$ is the weight of the sample at time $t$, and $m_\infty$ is the final weight of the sample.

The rate constant is described by the Arrhenius equation, Eq. 5,

$$k(\mathrm{T}) = A\exp\left(-\frac{E}{RT}\right) \quad (5)$$

where $A$ is a pre-exponential factor, $E$ is the activation energy, and $R$ (8.314 J mol$^{-1}$/K) is the gas constant. Function $f(\alpha)$ is expressed as Eq. 6,

$$f(\alpha) = (1-\alpha)^n \quad (6)$$

where $n$=1 is the reaction order in this study as Eq. 7.

$$f(\alpha) = (1-\alpha) \quad (7)$$

The heating rate of 10 K/ min is defined as Eq. 8:

$$\beta = \frac{\mathrm{d}T}{\mathrm{d}t} \quad (8)$$

The combination of Eqs. 3, 5, 7, and 8 gives:

$$\frac{\mathrm{d}\alpha}{\mathrm{d}T} = A\exp\left(-\frac{E}{RT}\right)(1-\alpha) \quad (9)$$

Equation 9 is the elementary expression for calculating kinetic parameters based on the TG data. The temperature of the sample was changed by a control, so the re-arrangement of Eq. 9 gives:

$$\frac{\mathrm{d}\alpha}{(1-\alpha)} = \frac{A}{\beta}\exp\left(-\frac{E}{RT}\right)\mathrm{d}T \quad (10)$$

Equation 8 is integrated by using the Coats–Redfern method, and thus, integrating both sides followed by taking the logarithm of the obtained equation is expressed as:

$$\ln\left[\frac{-\ln(1-\alpha)}{T^2}\right] = \ln\left[\frac{AR}{\beta E}\left(1-\frac{2RT}{E}\right)\right] - \frac{E}{RT} \quad (11)$$

Because the expression $\ln[AR/\beta E(1-2RT/E)]$ in Eq. 11 is essentially constant, re-arrangement of Eq. 11 gives:

$$\ln\left[\frac{-\ln(1-\alpha)}{T^2}\right] = \ln\left[\frac{AR}{\beta E}\right] - \frac{E}{RT} \quad (12)$$

Thus, a plot of $\ln[-\ln(1-\alpha)/T^2]$ against $1/T$ is a straight line with slope ($-E/R$) and intercept ($\ln[AR/\beta E]$), and the kinetic parameters were determined based on it.

## RESULTS AND DISCUSSION

This paper focuses on the characterization of the MCC pretreated by [Emim][$MeSO_3$]-$H_2O$ mixtures with solid acid catalyst Nafion®NR50 ([E]-$H_2O$-NR50 mixtures), and the pretreated microcrystalline cellulose (MCC) samples (where the sample code 90(20) indicates a ratio of $H_2O$ to IL set to 1:5 (20 wt%) at 90 °C) were subjected to a pyrolysis process with a focus on measuring the pyrolysis kinetics and gaseous products. The weight losses of all the pretreated MCC specimens were less than 10 wt%, and there were no gelation products in the pretreated samples.

### Characterization of MCC after Pretreatment

Common methods for the characterization of the crystalline cellulose structure are based on XRD and FTIR. The crystallinity index (Cr.I) was calculated from XRD curves

by the height ratio between the intensity of the crystalline peak and the total intensity. FTIR absorption gave some useful information related to the change of the hydrogen bonding during the crystal transformation during the IL-$H_2O$ pretreatment process.

In the pretreatment experiment, the mass ratio of the MCC powder to [Emim][$MeSO_3$], $H_2O$ and solid acid catalyst was set to 1 : 5 : (0.25, 0.5, 1, 2.5, and 5) : 0.5 at 90, 120, and 150 °C for 60 min. Then, the pretreated MCC was filtered and dried under vacuum for subsequent analysis and utilization. The XRD patterns of the pretreated MCC in [E]-$H_2O$-NR50 mixtures at 90 and 150 °C are shown in Fig. 1(a) and (b). The characterized crystalline structure, the change in the FTIR absorption, and the hydrogen bonding of the glucose units in cellulose are shown in Fig. 2(a) and (b) to elucidate the effect of the [E]-$H_2O$-NR50 mixtures on the MCC intrachain and interchain hydrogen bonding in ordered regions of the structure. The model in Fig. 2(c) represents the cellulose chains, showing the MCC structure and d-spacings of the 002 plane ($d_{002}$).

There was no transition from cellulose I to II under each experiment condition in this study. Therefore, no cellulose derivative was produced for subsequent utilization in these cases. Measurement of cellulose Cr.I by the XRD patterns provides a qualitative analysis of the amounts of amorphous cellulose and crystalline cellulose components in a pretreated sample. A clear shallow shoulder peak suggested that the arrangement of the cellulose chains was disturbed within the hydrogen-bonded sheets under each pretreatment temperature in Fig. 1(a) and (b). Meanwhile, the result of Cr.I clearly showed the change in the crystalline structure in pretreated MCC. The result of Cr.I ranged from 81 for sample 90(100) to 78 for sample 90(5) samples.

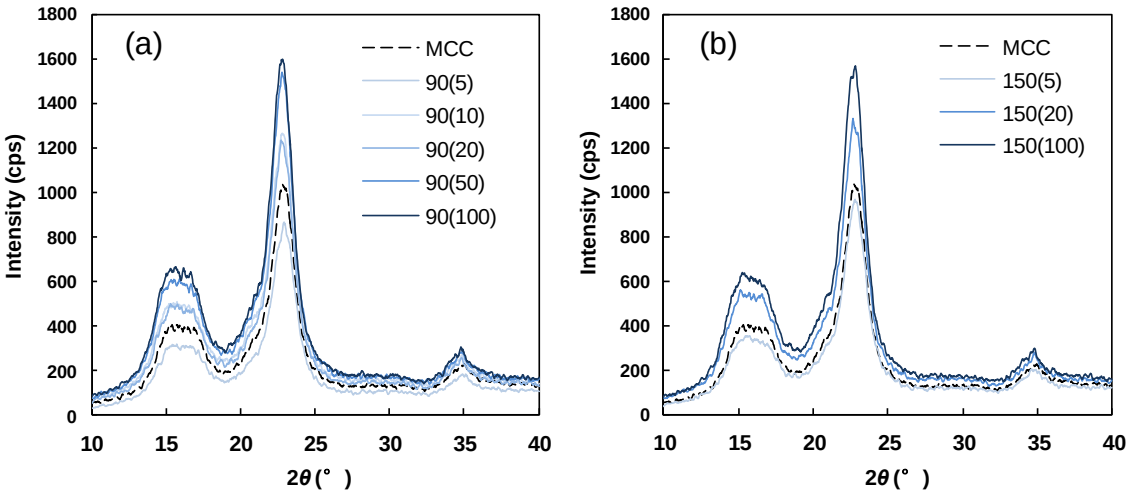


**Fig. 1.** X-ray diffractograms of pretreated MCC and untreated MCC at pretreatment temperatures of 90 °C (a) and 150 °C (b).

A simple height comparison could be expected to provide a reasonable estimate of the pretreated cellulose crystallinity parameters. However, variations in peak width also provide data on the crystallite size and/or d-spacing of the crystallites in MCC (Park *et al*. 2010). The *d*-spacing of the MCC samples pretreated at 90 °C calculated from the XRD profiles can be seen in Fig. 2(a). The results of $d_{002}$ were 0.388 (nm) for MCC and 0.392, 0.392, 0.391, 0.390, 0.390 (nm) for samples 90(5), 90(10), 90(20), 90(50), and 90(100), respectively. The increase in the average $d_{002}$ suggested that the pretreated MCC contained a looser cellulose structure than does the untreated MCC. Two major reasons may explain this behavior. The amorphous part of the cellulose was dissolved in the [E]-$H_2O$-NR50

mixtures, as observed in the Cr.I of sample 90(100), 81, which was higher than that of the untreated MCC samples. Meanwhile, it was reported that the pretreated MCC was distorted and transformed into a less-ordered intermediate structure, also a reflection Cr.I result (Cheng *et al*. 2012). The intrachain and interchain hydrogen bonding might have been disrupted by the [E]-$H_2O$-NR50 mixtures (Zhang *et al*. 2014). However, the hydrogen bonding forces became weaker than in the untreated MCC as a result of the pretreatment process could not be confirmed only by the XRD result.

The FTIR absorption data used to support the change in the hydrogen bonding in the pretreated MCC can be seen in Fig. 2(b). The band at 1033 $cm^{-1}$ is assigned as the CO at C-6, and the band at 1059 $cm^{-1}$ is assigned as the CO at C-3 (Kačuráková *et al*. 2002). Both of the bands exhibited increases in absorbance. This result indicated that the intrachain and interchain hydrogen bonding changed. The bands at 1235 $cm^{-1}$ assigned as the in plane C-OH at C6 decreased. The bands at 1337 $cm^{-1}$ assigned as the in plane C-OH at C2 and C3 also decreased and shifted to 1341 $cm^{-1}$ (Colom and Carillo 2002).

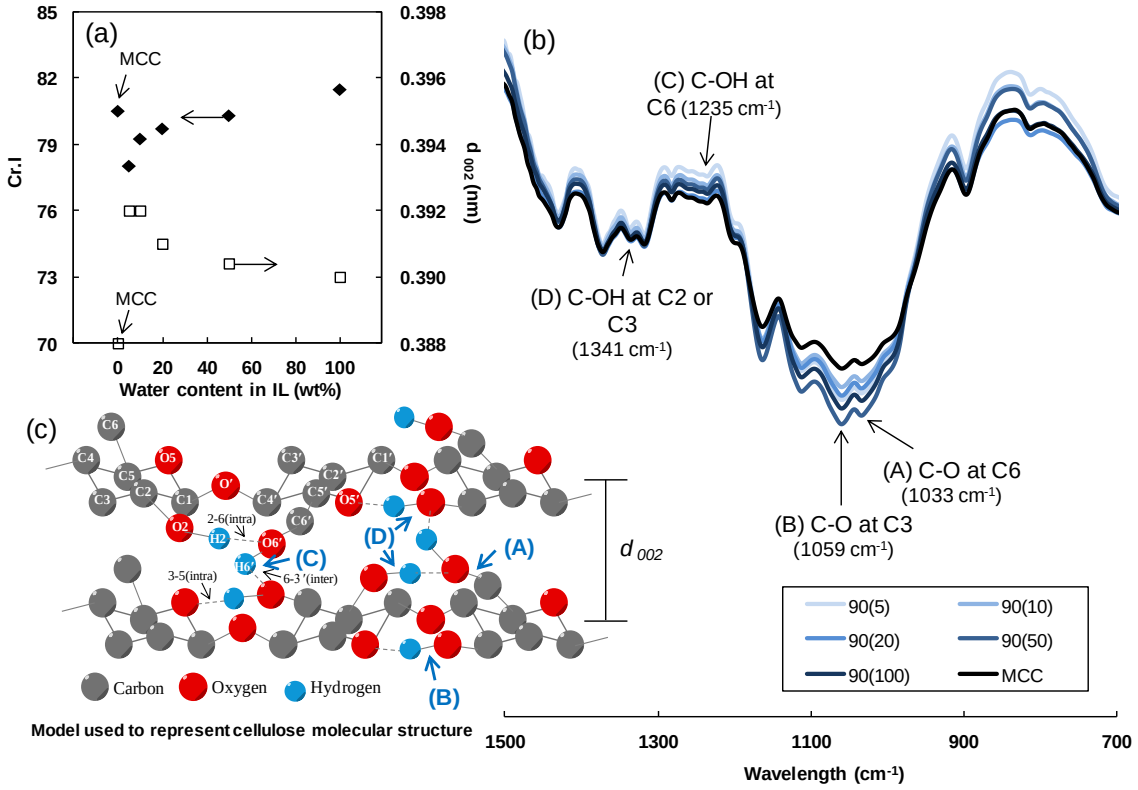


**Fig. 2.** The crystallinity index and d-spacings obtained from the XRD analysis (a), the FT-IR spectra (1500-700$cm^{-1}$) of pretreated MCC and untreated MCC (b) and the model used to represent the cellulose molecular structure (c)

The changes in hydrogen bonding led to an improved intermolecular force environment in the pretreated MCC. As a result, a looser crystalline structure was formed in the pretreated MCC. Previous solid acid catalyst studies provided insight into the mechanism of the release of protons from solid acid resin in an IL system (Dwiatmoko *et al*. 2010), explaining that a portion is released by ion-exchange with the cation of the IL, which could enhance the hydrolysis activity (Kim *et al*. 2010). This result suggests that the intrachain and interchain hydrogen bonding was disrupted by the released portion and the

anion of the IL from the [E]-$H_2O$-NR50 mixture system. Therefore, the smaller the water concentration in the [E]-$H_2O$-NR50 mixture, the lower the Cr.I results of the pretreated MCC that was obtained. It was confirmed that a looser cellulose crystalline structure was formed.

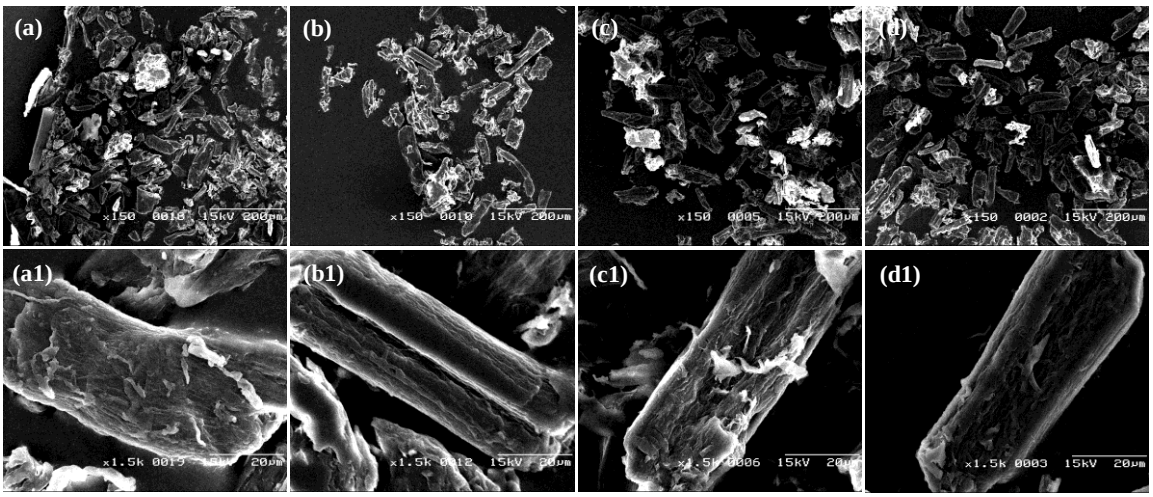


**Fig. 3.** SEM was used to observe the untreated MCC (a), sample 90(20) (b), sample 120(20) (c), and sample 150(20) (d) at different magnifications

The surface structure of the MCC samples pretreated at 90 °C, 120 °C, and 150 °C was carefully observed by SEM in Fig. 3. Two main changes can be concluded. First, the amount of irregularly shaped cellulose particles decreased. Second, a visual trend is shown in the SEM results in Fig. 3(b1), (c1) and (d1), where the MCC samples pretreated with [E]-$H_2O$-NR50 mixtures showed obvious cracks on their surfaces leading to an increase in the surface area of the pretreated MCC. However, there were no obvious differences between the different pretreatment temperatures. The changes in crystallinity, $d_{002}$ plane and surface structure were found to severely affect the thermal stability of the cellulose (Poletto *et al*. 2012).

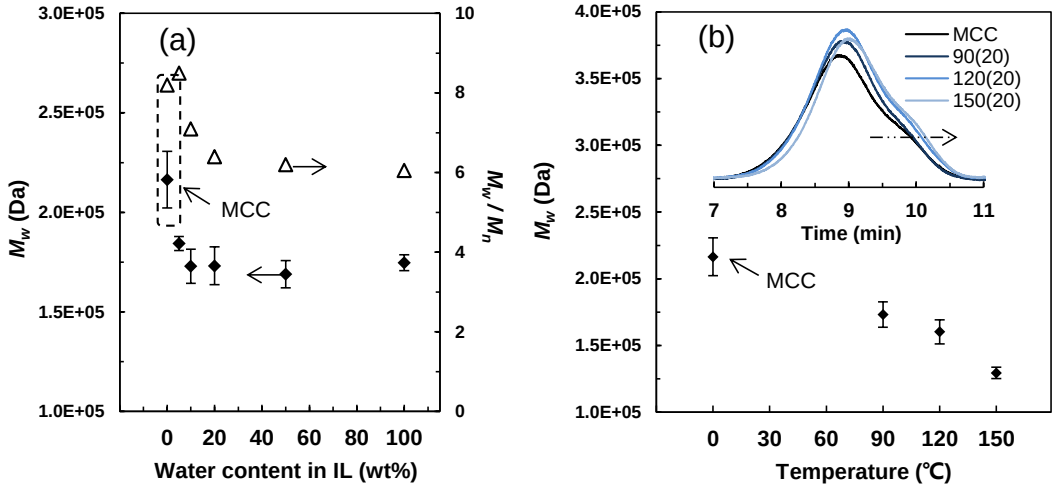


**Fig. 4.** GPC result of pretreated MCC and untreated MCC with different amounts of $H_2O$ in the mixture (a) and different pretreatment temperatures (b)

The GPC result showed that the average molecular weight decreased after pretreatment (see sample 90(100)), as shown in Fig. 4(a). However, the average molecular weight increased with the increasing concentrations of the ionic liquid. In the other words, the lower molecular weight part of the MCC more easily dissolved in the mixture system (Wang *et al*. 2014). The average molecular weight decreased with the increasing pretreatment temperature, as shown in Fig. 4(b). Therefore, the manner in which the pretreated cellulose affects the pyrolysis process, char yield and gaseous products is equally interesting.

## Pyrolysis of Pretreated MCC

The char yields obtained from pyrolysis of pretreated MCC at 900 °C and the $DTG_{max}$ values calculated from the TG curve are shown in Fig. 5(a). The kinetic parameters for MCC pyrolysis are shown in Fig. 5(b) and reflect the degradation of the total pretreated sample under different pretreatment conditions.

The purpose of this study was that the IL-$H_2O$ mixture pretreated MCC be subjected to a pyrolysis process. For lignocellulosic biomass, cellulose mainly contributes to the liquid and gas yields. In this study, a mixed $SiO_2$+$Ca(OH)_2$ catalyst was used to transform the intermediate product into gaseous products. Figure 6(a) shows that the char yields obtained from the pretreated samples at 900 °C were significantly decreased compared to that from the untreated MCC. This indicates that greater liquids yield and/or gas yields could be obtained. The amount of char yield was different in samples such as 90(5) and 150(5), which were pretreated in higher concentrations of ILs. Once again, the crystallinity index, crystallite size and surface structure can affect the thermal stability of the cellulose. Therefore, this result indicated that no variation in the crystallinity structure occurred in samples pretreated with an excess amount of water *i.e.*, sample 90(50) and sample 90(100)). The effect of the [E]-$H_2O$-NR50 mixture systems on MCC was limited due to the excess amount of water, even at a higher pretreatment temperature (i.e., sample 150(100)). The $DTG_{max}$ value increased when less water was loaded in the [E]-$H_2O$-NR50 mixtures system. From the slope of Eq (12), the apparent activation energy can be calculated, as is shown in Fig. 5(b).

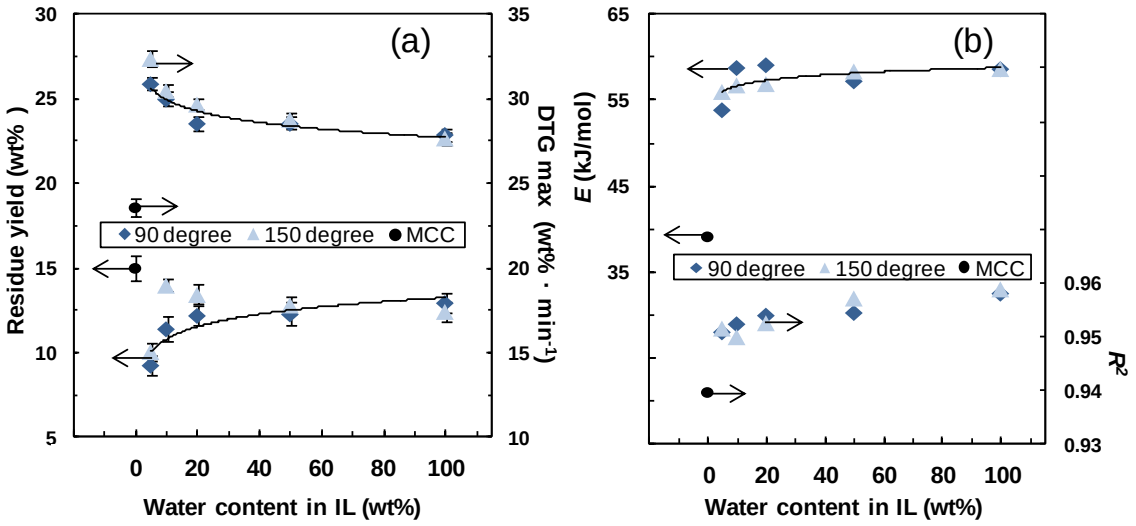


**Fig. 5.** Yields of char and DTGmax (a) and kinetic parameters (b) obtained from pyrolysis of pretreated MCC under varying pretreatment condition

The temperature showed an approximately linear increase with a heating rate of 10 °C / min under argon gas in the range of 280 to 380 °C for pyrolysis. The activation energy had high linear coefficients of determination ($R^2$) in the range from 0.9516 to 0.9586. The average values of the activation energy for the pyrolysis varied slightly. The average activation energy values obtained for pyrolysis of samples 90(5), 90(10), 90(20), 90(50), and 90(100) were 53.9, 58.8, 59.1, 57.3, and 58.7 kJ/mol, respectively. The value of the activation energy obtained in the pyrolysis of pretreated MCC samples at different pretreatment temperatures were in a similar range. A lower activation energy (39.2 kJ/mol) was observed in untreated MCC. These result indicated that the decrease of the char yield was correlated with higher activation energy. The higher activation energy calculated for the pretreated MCC pyrolysis could therefore be associated with the lower char formation (Cho *et al*. 2010).

The TG curves of the MCC and 90(5)-90(100) samples that differed in the ratio of the water content to the ionic liquid are shown in Fig. 6(a). The DTG curves of the 90(5)-90(100) samples are plotted in Fig. 6(b), which was used to compare the degradation rate of the pretreated MCC. With the temperature increasing further, the TG profile of the pretreated MCC showed an obvious peak.

The DTG peak of the pretreated MCC was lower than that of the untreated MCC. Poletto *et al*. (2012) reported that the thermal decomposition of cellulose shifted to higher temperatures due to the increasing crystallinity index and crystallite size in a biomass sample case. In this study, the results showed that the thermal decomposition of pretreated MCC was shifted to lower temperatures with the decreasing crystallinity index. A higher $DTG_{max}$ result of cellulose was also obtained. On the other hand, the crystallinity index was not only related to the degradation rate of the pretreated MCC but also to the thermal decomposition temperature.

A lower amount of hydrogen bonding between neighboring cellulose chains results from a looser cellulose crystalline structure, which can lead to a lower crystallinity index and thermal stability. Zickler *et al*. (2007) also reported that the thermal decomposition of cellulose is mainly via a thermally activated decrease of the cellulose diameter.

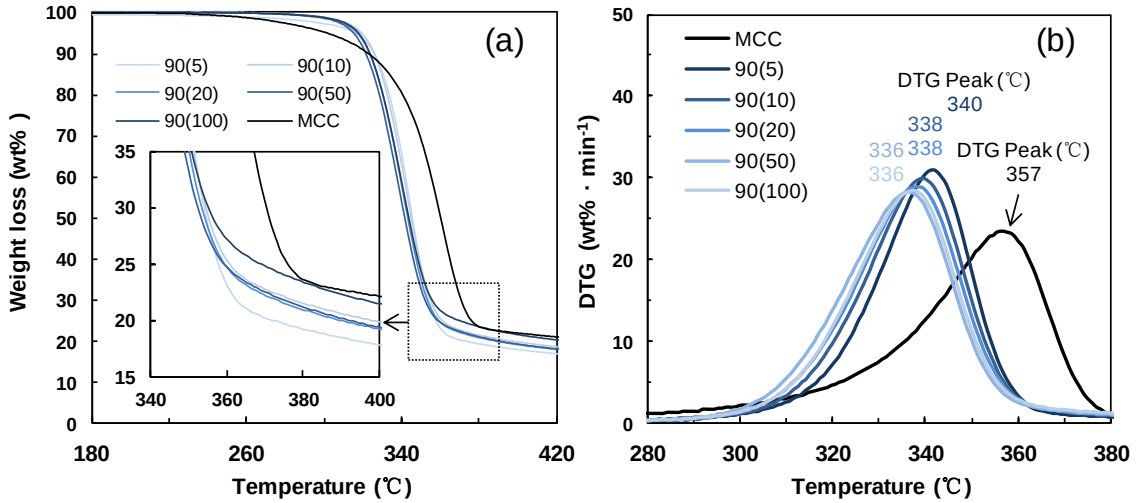


**Fig. 6.** TG curve (a), DTG curve and DTG peak (b) obtained from pyrolysis of pretreated MCC

## Product Yields of the Pyrolysis Process

The laboratory experimental methods used in this study are shown in Fig. 7(a). The total amounts of collected char, liquid, and gas products are shown in Fig. 7(b). The most common mechanism for cellulose pyrolysis is that the initial reaction is an induction or activation step, the intermediate product of which is defined as active cellulose (Banyasz *et al*. 2001). After this process, the intermediate product is decomposed by a pair of competing pathways.

One of these reactions produces a liquid product (of tar and water), and the other generates char and gas products. The formation of char becomes a dominant reaction path depending on heating rates and temperatures (Yang *et al*. 2006). In this study, the pretreated MCC tends to release lower gas products and char products. However, sample 90(20) showed that the mixed $SiO_2$+$Ca(OH)_2$ catalyst could transfer more intermediate product into the gas product. Therefore, the composition of the main pyrolysis products might significantly relate to the sample physical-chemical characteristics.

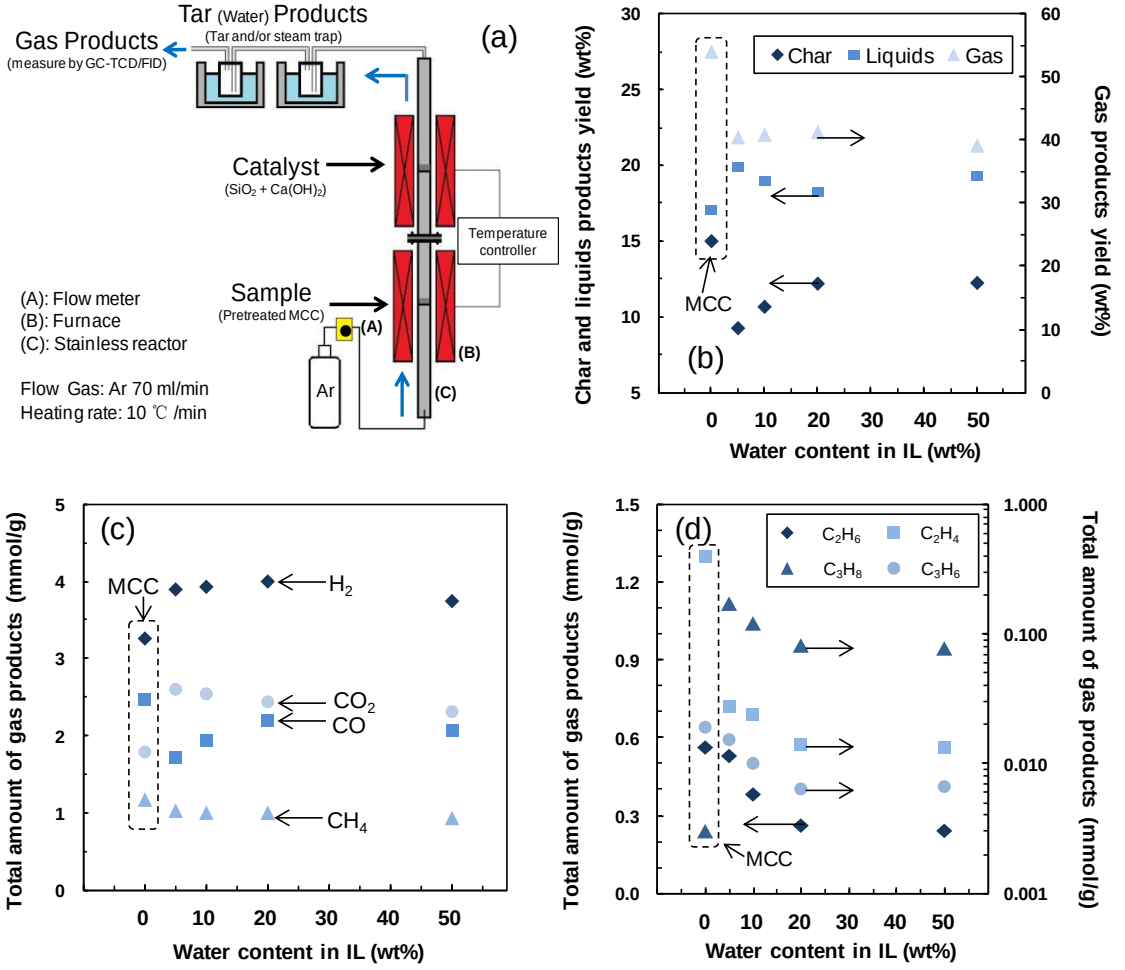


**Fig. 7.** The experimental procedure of the pyrolysis device system (a), the overall distribution of char, liquid and gas products obtained from the pyrolysis of MCC (b), total amount of main gas product obtained from the pyrolysis of MCC, pretreated sample (c), total amount of hydrocarbon products (d).

**Table. 1. The Yields of Char, Liquid, and Gas Products Obtained from the Pyrolysis of Pretreated Sample at Different Pretreatment Temperatures**

| Sample code | Majority products (wt. %) | | | Gas product (mmol/g) | | | | |
|---|---|---|---|---|---|---|---|---|
| | Char | Liquid | Gas | $H_2$ | CO | $CH_4$ | $CO_2$ | Hydrocarbons |
| MCC | 15.0 | 17.1 | 54.1 | 3.26 | 2.46 | 1.17 | 1.79 | 0.97 |
| 90(20) | 11.4 | 18.3 | 41.6 | 4.00 | 2.19 | 1.00 | 2.44 | 0.46 |
| 150(20) | 13.5 | 19.5 | 47.3 | 4.39 | 2.76 | 1.09 | 2.63 | 0.51 |

The pyrolysis of the samples was carried out using the heating rate of 10 °C / min under argon gas. The pyrolysis process was in a range from 180 to 900 °C. The measurement of gas products was carried out every 80 °C. The gas species distributions were quite similar for the cases of loading mixed $SiO_2$+$Ca(OH)_2$ as the catalyst. The total yields of $H_2$, CO, $CH_4$, and $CO_2$ calculated at 900 °C are shown in Fig. 7(c). Some hydrocarbons ($C_2H_6$, $C_2H_4$, $C_3H_8$ and $C_3H_6$) are shown in Fig. 7(d).

The gas product from sample 90(20) contained 3.995 mmol/g(sample) of $H_2$, 2.192 mmol/g(sample) of CO, 0.997 mmol/g(sample) of $CH_4$, and 2.436 mmol/g(sample) of $CO_2$. The gas product from the unpretreated MCC contained 3.256 mmol/g(sample) of $H_2$, 4.924 mmol/g(sample) of CO, 1.168 mmol/g(sample) of $CH_4$, and 1.785 mmol/g(sample) of $CO_2$. The changing trend of the $H_2$ concentration can reflect the extent of the secondary reactions (Dai *et al*. 2000).

No more $H_2$ gas was observed at a higher temperature (＞500°C). Therefore, the greater $H_2$ generation could be related to the pretreatment process, while the yield of CO gas obtained from the pretreated samples was decreased. The $CO_2$ content increased as the hydrocarbons decreased, including $CH_4$. This might have been caused by different operating conditions and the sample physical-chemical characteristics (Scott *et al*. 1988). In addition, the pretreated MCC subjected to a pyrolysis process at different temperatures are listed in Table. 1. It was found that the yield of the $H_2$ gas obtained from the pretreated sample was higher than that from the untreated MCC.

Overall, the pretreatment process was studied with respect to their products being subjected to a pyrolysis process. Thus, the relevance of the pretreatment process and pyrolysis process should be considered. First, the intrachain and interchain hydrogen bonding was disrupted by [E]-$H_2O$-NR50 mixtures. The disordered crystalline structure led to a decreased amount of Cr.I, and weaker hydrogen bonding forces in the cellulose crystallite structure. This resulted from a looser cellulose structure, which led to lower crystallinity and thermal stability, as observed in all pretreated MCC samples. Second, the higher activation energy confirmed in the pretreated MCC could be associated with the lower char formation. As a result, more active cellulose should be formed. However, the total amount of gaseous products also decreased. Therefore, the liquid products should be important for future study. Third, hydrogen-rich gas was obtained from the pyrolysis of pretreated MCC, as observed in all pretreated MCC samples including the pretreated MCC using the low concentration IL-$H_2O$ mixture systems. Therefore, a low water content in IL-$H_2O$ mixtures for MCC pretreatment might not be a necessary condition for the pyrolysis process.

## CONCLUSIONS

In this work, microcrystalline cellulose (MCC) samples pretreated by [Emim][$MeSO_3$]-$H_2O$ mixtures with the solid acid catalyst Nafion®NR50 were studied for their application in a pyrolysis process. A lower amount of hydrogen bonding between neighboring cellulose chains resulting from a looser cellulose crystalline structure could lead to a lower crystallinity index and thermal stability. The higher activation energy calculated from the pretreated MCC pyrolysis could be associated with the lower char formation. The amount of hydrogen gas obtained from the pyrolysis of the pretreated sample was higher than that of the MCC, while the yield of char was decreased.

## ACKNOWLEDGMENTS

The research was supported by the special funds for Basic Researches (B) (No. 22303022) of Grant-in-Aid Scientific Research of the Japanese Ministry of Education, Culture, Sports, Science and Technology (MEXT), Japan.

## REFERENCES CITED

Bahcegul, E., Apaydin, S., Haykir, N. I., Tatlic, E., and Bakir, U. (2012). "Different ionic liquids favour different lignocellulosic biomass particle sizes during pretreatment to function efficiently," *Green. Chem.* 14, 1896-1903. DOI: 10.1039/C2GC35318K

Banyasz, J. L., Li, S., Lyons-Hart, J. L., and Shafer, K. H. (2001). "Cellulose pyrolysis: The kinetics of hydroxyacetaldehyde evolution," *J. Anal. Appl. Pyrolysis.* 57, 223-248. DOI:10.1016/S0165-2370(00)00135-2

Brandt, A., Ray, M. J., To, T. Q., Leak, D. J., Murphybc, R. J. and Welton, T. (2011). "Ionic liquid pretreatment of lignocellulosic biomass with ionic liquid-water mixtures," *Green. Chem*, 13, 2489-2499. DOI: 10.1039/C1GC15374A

Brandt, A., Gräsvik, J., Halletta, J. P., and Welton, T. (2013). "Deconstruction of lignocellulosic biomass with ionic liquids," *Green. Chem.* 15, 550-583. DOI: 10.1039/C2GC36364J

Chen, Q., Endo, T., and Wang, Q. (2015). "Characterization of bamboo after ionic liquid-$H_2O$ pretreatment for the pyrolysis process," *BioResources* 10(2), 2797-2808, DOI: 10.15376/biores.10.2.2797-2808

Cheng, G., Varanasi, P., Arora, R., Stavila, V., Simmons, B. A., Kent, M. S., and Singh. S. (2012). "Impact of ionic liquid pretreatment conditions on cellulose crystalline structure using 1-ethyl-3-methylimidazolium acetate," *J. Phys. Chem. B.* 116 (33), 10049-10054. DOI: 10.1021/jp304538v

Cho, J., Davis, J. M., and Huber, G. W. (2010). "The intrinsic kinetics and heats of reactions for cellulose pyrolysis and char formation," *ChemSusChem*. 3, 1162-1165. DOI: 10.1002/cssc.201000119

Colom, X., and Carrillo, F. (2002). "Crystallinity changes in lyocell and viscose-type fibres by caustic treatment," *Eur. Polym. J*. 38, 2225-2230. DOI:10.1016/S0014-3057(02)00132-5

Dai, X., Wu, C., Li, H., and Chen, Y. (2000). "The fast pyrolysis of biomass in CFB reactor," *Energy Fuels*. 14(3), 552-557. DOI: 10.1021/ef9901645

Dwiatmoko, A. A., Choi, J. W., Suh, D. J., Suh, Y. W., and Kung, H. H. (2010). "Understanding the role of halogen-containing ionic liquids in the hydrolysis of cellobiose catalyzed by acid resins," *Appl. Catal. A: Gen*. 387, 209-214. DOI:10.1016/j.apcata.2010.08.032

Heym, F., Etzold, B. J. M., Kern, C., and Jess A. (2011). "Analysis of evaporation and thermal decomposition of ionic liquids by thermogravimetrical analysis at ambient pressure and high vacuum," *Green Chem*. 13, 1453-1466. DOI:10.1039/C0GC00876A

Hou, X. D., Li, N., and Zong, M. H. (2013). "Facile and simple pretreatment of sugar cane bagasse without size reduction using renewable ionic liquids-water mixtures," *ACS. Sustainable. Chem. Eng*. 1, 519-526. DOI: 10.1021/sc300172v

Kačuráková, M., Smith, A. C., Gidley, M. J., and Wilson, R. H. (2002). "Molecular interactions in bacterial cellulose composites studied by 1D FT-IR and dynamic 2D FT-IR spectroscopy," *Carbohydr. Res*. 337, 1145-1153. DOI:10.1016/S0008-6215(02)00102-7

Kim, S. J., Dwiatmoko, A. A., Choi, J. W., Suh, Y. W., Suh, D. J., and Oh, M. (2010). "Cellulose pretreatment with 1-n-butyl-3-methylimidazolium chloride for solid acid-catalyzed hydrolysis," *Bioresour. Technol*. 101, 8273-8279. DOI:10.1016/j.biortech.2010.06.047

Li, C., Knierim, B., Manisseri, C., Arora, R., Scheller, H. V., Auer, M., Vogel, K. P., Simmons, B. A., and Singh, S. (2010). "Comparison of dilute acid and ionic liquid pretreatment of switchgrass: biomass recalcitrance, delignification and enzymatic saccharification," *Bioresour. Technol.* 101 (13), 4900-4906. DOI: 10.1016/j.biortech.2009.10.066

López-Pastor, M., Ayora-Cañada, M. J., Valcárcel, M., and Lendl, B. (2006). "Association of methanol and water in ionic liquids elucidated by infrared spectroscopy using two-dimensional correlation and multivariate curve resolution," *J. Phys. Chem. B*, 110(22), 10896-10902. DOI: 10.1021/jp057398b

Gericke, M., Trygg, J., and Fardim, P. (2013). "Functional cellulose beads: Preparation, characterization, and applications," *Chem. Rev*. 113(7), 4812-4836. DOI: 10.1021/cr300242j

Mazza, M., Catana, D. A., Vaca-Garcia, C., and Cecutti, C. (2009). "Influence of water on the dissolution of cellulose in selected ionic liquids," *Cellulose*. 16(2), 207-215. DOI 10.1007/s10570-008-9257-x

Mosier, N., Wyman, C., Dale, B., Elander, R., Lee, Y. Y., Holtzapple, M., and Ladisch, M. (2005). "Features of promising technologies for pretreatment of lignocellulosic biomass," *Bioresour. Technol*, 95, 673-696. DOI:10.1016/j.biortech.2004.06.025

Olivier-Bourbigou, H., Magna, L., and Morvan, D. (2010). "Ionic liquids and catalysis: Recent progress from knowledge to applications," *Appl. Catal. A-Gen*. 373, 1-56. DOI:10.1016/j.apcata.2009.10.008

Park, S., Baker1, J. O., Himmel1, M. E., Parilla, P. A., and Johnson, D. K. (2010). "Cellulose crystallinity index: Measurement techniques and their impact on interpreting cellulase performance," *Biotechnol. Biofuels*. 3(10).

Pinkert, A., Marsh, K. N., Pang, S., and Staiger, M. P. (2009). "Ionic liquids and their interaction with cellulose," *Chem. Rev*, 109(12), 6712-6728. DOI:10.1021/cr9001947

Poletto, M., Zattera, A. J., Forte, M. M. C., and Santana, R. M. C. (2012). "Thermal decomposition of wood: Influence of wood components and cellulose crystallite size," *Bioresour. Technol.* 109, 148-153. DOI:10.1016/j.biortech.2011.11.122

Rinaldi, R., Palkovits, P., and Schüth, F. (2008). "Depolymerization of cellulose using solid catalysts in ionic liquids," *Angew. Chem. Int. Edit*. 47, 8047- 8050. DOI: 10.1002/anie.200802879

Scott, D. S., Piskorz, J., Bergougnou, M. A., Graham, R., and Overend, R. P. (1988). "The role of temperature in the fast pyrolysis of cellulose and wood," *Ind. Eng. Chem. Res.* 27, 8-15. DOI: 10.1021/ie00073a003

Sun, N., Rahman, M., Qin, Y., Maxim, M. L., Rodríguez, H., and Rogers, R. D. (2009). "Complete dissolution and partial delignification of wood in the ionic liquid 1-ethyl-3-methylimidazolium acetate," *Green Chem.* 11, 646-655. DOI: 10.1039/B822702K

Swatloski, R. P., Spear, S. K., Holbery, J. D., and Rogers, R.D. (2002). "Dissolution of cellulose with ionic liquids," *J. Am. Chem. Soc*. 124, 4974-4975. DOI: 10.1021/ja025790m

Wada, M., Okano, and T., Sugiyama, J. (2001). "Allomorphs of native crystalline cellulose I evaluated by two equatorial d-spacings," *J. Wood. Sci*. 47(2), 124-128. DOI: 10.1007/BF00780560

Wang, Q., Chen, Q., Mitsumura, N., and Animesh, S. (2014). "Behavior of cellulose liquefaction after pretreatment using ionic liquids with water mixtures," *J. Appl. Polym. Sci.* 131, 40255-40263. DOI: 10.1002/app.40255

Yang, H., Yan, R., Chen, H., Lee, D. H., Liang, D. T., and Zheng, C. (2006). "Pyrolysis of palm oil wastes for enhanced production of hydrogen rich gases," *Fuel Process. Technol.* 87(10), 935–942. DOI: 10.1016/j.fuproc.2006.07.001

Zhang, J., Wang, Y., Zhang, L., Zhang, R., Liu, G., and Cheng. G. (2014). "Understanding changes in cellulose crystalline structure of lignocellulosic biomass during ionic liquid pretreatment by XRD," *Bioresour. Technol.* 151, 402-405. DOI:10.1016/j.biortech.2013.10.009

Zhang, Z. Y., Haraab, I. M. O'., and Doherty, W. O. S. (2013). "Effects of pH on pretreatment of sugarcane bagasse using aqueous imidazolium ionic liquids," *Green. Chem.* 15, 431-438. DOI: 10.1039/C2GC36084E

Zickler, G.A., Wagermaier, W., Funari, S.S., Burghammer, M., and Paris, O. (2007). "In situ X-ray diffraction investigation of thermal decomposition of wood cellulose," *J. Anal. Appl. Pyrolysis.* 80, 134-140. DOI:10.1016/j.jaap.2007.01.011

Article submitted: July 23, 2015; Peer review completed: September 20, 2015; Revised version received and accepted; September 27, 2015; Published: November 10, 2015.
DOI: 10.15376/biores.11.1.159-173